Chemical Science

ROYAL SOCIETY OF CHEMISTRY

EDGE ARTICLE

View Article Online
View Journal | View Issue

Cite this: *Chem. Sci.*, 2024, **15**, 2062

All publication charges for this article have been paid for by the Royal Society of Chemistry

The fate of the contact ion pair determines the photochemistry of coumarin-based photocleavable protecting groups†

Albert Marten Schulte, ‡[a] Georgios Alachouzos, ‡*[a] Wiktor Szymanski *[ab] and Ben L. Feringa *[a]

Photocleavable protecting groups (PPGs) enable the precise spatiotemporal control over the release of a payload of interest, in particular a bioactive substance, through light irradiation. A crucial parameter that determines the practical applicability of PPGs is the efficiency of payload release, largely governed by the quantum yield of photolysis (QY). Understanding which parameters determine the QY will prove crucial for engineering improved PPGs and their effective future applications, especially in the emerging field of photopharmacology. The Contact Ion Pair (CIP) has been recognized as an important intermediate in the uncaging process, but the key influence of *its fate* on the quantum yield has not been explored yet, limiting our ability to design improved PPGs. Here, we demonstrate that the CIP escape mechanism of PPGs is crucial for determining their payload- and solvent-dependent photolysis QY, and illustrate that an intramolecular type of CIP escape is superior over diffusion-dependent CIP escape. Furthermore, we report a strong correlation of the photolysis QY of a range of coumarin PPGs with the DFT-calculated height of all three energy barriers involved in the photolysis reaction, despite the vastly different mechanisms of CIP escape that these PPGs exhibit. Using the insights obtained through our analysis, we were able to predict the photolysis QY of a newly designed PPG with particularly high accuracy. The level of understanding of the factors determining the QY of PPGs presented here will move the ever-expanding field of PPG applications forward and provides a blueprint for the development of PPGs with QYs that are independent of payload-topology and solvent polarity.

Received 26th October 2023
Accepted 5th January 2024

DOI: 10.1039/d3sc05725a

rsc.li/chemical-science

Introduction

Using light as a stimulus to control chemical or biological processes confers many distinct advantages, which include: (i) spatiotemporal control of the desired process within a complex (bio)chemical system; (ii) milder conditions of photochemical processes, when compared to thermal or chemically initiated processes; (iii) the chemically non-contaminating and non-invasive nature of light.[1–5] To enable photochemical control, efficient molecular tools are required that absorb light and selectively execute the desired chemical process.

One cornerstone class of such photochemical tools are photolabile protecting groups (PPGs)[6–13] that enable the use of light to control one of the simplest chemical processes: *the breaking of a covalent sigma bond*. Through enabling this primary photochemical process, PPGs have found applications as protecting groups of functional moieties in organic synthesis of small molecule building blocks and in total syntheses of natural products, and have shown to be highly versatile for the release of (bioactive) payloads in molecular biology, materials science, and in photopharmacology.[14–23]

One of the most widely used classes of PPGs is that of the heterolytic PPGs, containing among others coumarin-[24–28] and BODIPY-PPGs.[29–32] Their shared mechanism of payload release relies on excited state heterolysis of the bond between the payload and the α-carbon of the PPG (Fig. 1a, k_1). In this process, a contact ion pair (CIP) intermediate is formed, in which the positive charge is located on the α-carbon of the PPG, and the negative charge on the payload. The initial heterolysis step is reversible, and – depending on its stability – the CIP will either recombine to reform the substrate (Fig. 1a, k_{-1}), or react further through diffusion of the CIP and trapping by the solvent (such as water, Fig. 1a, k_2) to release the payload and the PPG-alcohol.[33–36]

Since the applications of PPGs have exponentially expanded in the last decade,[37–40] much of their development has focused on tuning their efficiency of payload release,[41,42] which hinges

[a]*Centre for Systems Chemistry, Stratingh Institute for Chemistry, Faculty for Science and Engineering, University of Groningen, Nijenborgh 4, 9747 AG Groningen, The Netherlands. E-mail: alachouzos.georgios@gmail.com; w.c.szymanski@rug.nl; b.l.feringa@rug.nl*

[b]*Department of Radiology, Medical Imaging Center, University Medical Center Groningen, University of Groningen, Hanzeplein 1, 9713 GZ Groningen, The Netherlands*

† Electronic supplementary information (ESI) available. See DOI: https://doi.org/10.1039/d3sc05725a

‡ These authors contributed equally to this work.

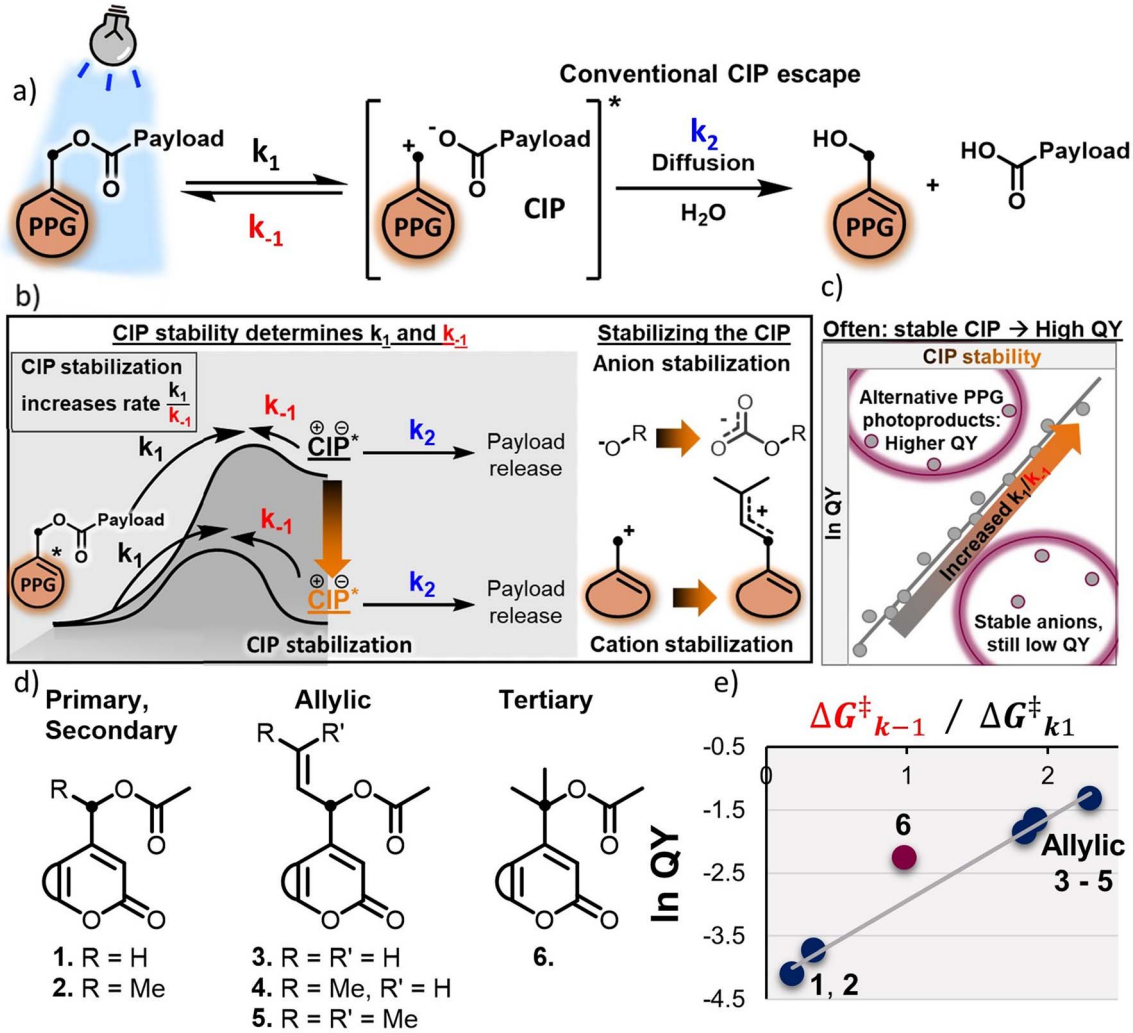

Fig. 1 (a) Mechanism of photocleavage of heterolytic PPGs, showing the initial reversible heterolysis step to form the CIP intermediate and the conventional diffusion-based CIP escape that together result in payload release. (b) Schematic representation of the energy diagram of photocleavage of coumarin uncaging, illustrating the two general strategies of stabilizing the CIP intermediate: anion and cation stabilization. (c) Schematic representation of the relationship between CIP stability and QY of uncaging for heterolytic PPGs, illustrating the outliers that are sometimes observed (see text). (d) Coumarin PPGs with improved cation stability studied recently by our group. The fused aromatic ring of the coumarin chromophore is abbreviated by a semicircle. (e) Correlation of photolysis QY and DFT-calculated k_{-1} over k_1 barrier height of coumarins **1–6**.

on the mathematical product $\varepsilon \times \Phi$, where the molar absorptivity ε defines *the efficiency of photon absorption* at a given irradiation wavelength and a given PPG concentration, and where the quantum yield of photolysis (QY, Φ) defines *the chance that a PPG in the excited state will release the payload* (instead of returning to the ground state through other processes). The QY of a PPG is a crucial parameter, as it describes the ability of the PPG to carry out the very function it was designed for. A low QY significantly hinders the application of PPGs in fields where light-delivery is challenging, such as photopharmacology, where insufficient uncaging efficiency would require prolonged irradiation or use of higher intensity light, which is not feasible in a clinical setting.[43] Furthermore, for the successful application of PPGs in fields that require near-instant release of a payload, such as time-resolved crystallography or materials chemistry, a high QY is crucial.[44,45]

A typical approach to increase the QY of heterolytic PPGs is to alter the nature of the leaving group, *e.g.* by employing a less Brønsted basic payload that efficiently stabilizes its incipient anionic charge in the CIP, increasing the ratio of the k_1/k_{-1} rates and driving the uncaging process in the forward direction (Fig. 1b, CIP stabilization through anion stabilization),[33,46] however it has to be noted that this way of QY engineering is unique to heterolytic PPGs, and does not necessarily work for PPGs that rely on different mechanisms of photolysis.[47] When using this approach, often a correlation can be found between the pK_a of the payload and the uncaging QY, with PPGs bearing payloads with lower pK_a featuring higher QYs (Fig. 1c).[33] However, this strategy involves direct chemical alterations of the payload, potentially affecting the desired application (for example, by diminishing the bioactivity of a biological molecule transiently "photocaged" by the PPG).

Recently, our group reported on a novel strategy to boost the QY of heterolytic PPGs by stabilizing the generated PPG cationic component of the CIP *via* hyperconjugation and/or positive charge delocalization (Fig. 1b, CIP stabilization through cation stabilization and Fig. 1d, compounds **3–6**). Stabilization of the CIP was thus achieved by retarding the unproductive k_{-1} process, and allowing the CIP to undergo the productive chemical process k_2 (Fig. 1b).[48] In addition, we found a clear correlation between the experimentally recorded QY and the TD-DFT-calculated barriers of photolysis (k_1) and CIP recombination (k_{-1}), offering a strong computational predictive method for the design of efficient PPGs (Fig. 1e).

In our continuous effort towards understanding the full spectrum of chemical parameters that affect PPG QY, we summarize two puzzling observations from our own and other research groups' studies:

(1) Stabilizing the incipient anionic payload component of the CIP by employing a more weakly basic payload (*i.e.* with a stronger conjugate acid) does not always result in a more efficient uncaging process (Fig. 1c, stable anions).[33,46] Instead, *a complex interplay of payload conjugate acid pK_a and overall payload topology (size, lipophilicity, etc.), and the polarity of the employed solvent*[49] *all appear to influence QY.*

(2) Stabilizing the incipient cationic PPG component of the CIP as a tertiary cation (compound **6**, *i.e.* methyl-*versus* allyl-substituted cations) resulted in a deviation from the correlation between experimental PPG QY and TD-DFT-calculated k_{-1}/k_1 energy barrier ratio, *showing a higher than expected QY (Fig. 1e), and yielding a different product of PPG release: an alkene, which is a result of deprotonation instead of the usual solvent-trapped alcohol photoproduct.*[48] Similarly, coumarin- or BODIPY-PPGs engineered to give different photoproducts (*e.g. via* intramolecular capture of the cationic PPG component of the CIP) *also appear follow this general trend of increased QY* (Fig. 1c, alternative photoproducts).[42,50,51]

As a consequence of these puzzling observations, we hypothesized that the rate of CIP formation k_1 and the rate of unproductive CIP recombination k_{-1}, though critical parameters in engineering efficient QYs of PPGs,[34,48] do not provide the full picture for overall PPG photolysis efficiency. Therefore, we set out to further investigate the productive process k_2 that allows the payload to escape the CIP. While the crucial influence of the CIP intermediate itself on PPG photolysis has been recognized,[33,34,37,48] its fate has so far not been explored as a key PPG design parameter.

Herein we outline the limitations of current PPG QY optimization methods and provide a robust framework for the future QY engineering methods for these valuable photochemical tools. We demonstrate the significant importance of the *fate of the CIP* in determining solvent- and payload-dependent photochemical properties, and showcase factors other than CIP stability that influence the QY of heterolytic diffusion-dependent PPGs. Furthermore, we provide more detailed insight in the photochemical behavior of the previously reported class of di-methyl-substituted coumarin PPGs **6**, and demonstrate their unique photochemical properties with an overall uncaging mechanism independent of the molecular topology of the payload and the nature of employed solvent.

A photolysis mechanism independent of diffusion

Typically, irradiation of coumarin PPGs in water yields the payload and coumarin-derived alcohols, which are formed by water trapping of the incipient cation of the CIP. Primary, secondary and allylic coumarins **1–5** all follow this conventional mechanism (Fig. 2a). The formation of the alcohols from the CIP is thought to arise in two steps: diffusion of the CIP into a solvent separated ion pair, followed by water capture of the cation.[33,52] It has previously been speculated that an alternative mechanism of CIP escape could be the direct trapping of the cation by water molecules present at the inner surface of the CIP, circumventing the need for diffusion.[34] The extent to which these two processes contribute to the overall k_2 so far has remained unclear. However, if k_2 is largely dependent on diffusion of the ions, it is expected to be strongly influenced by factors including (1) *the polarity of the solvent* and (2) *the size and hydrophobicity of the molecules constituting the CIP.* These factors would arguably affect the diffusion energy barrier (Fig. 2a, $\Delta G_2^{\ddagger}$), with the use of low polarity solvents and larger payloads leading to the increase of this barrier and reducing the diffusion rate.

At the onset of this study, we hypothesized that the newly observed alkene photoproduct in the photochemical release of a model payload from **6** was due to an alternative CIP escape mechanism k_2, that relied on deprotonation of the incipient coumarin cation from the payload anion (Fig. 2b). In the tertiary coumarin **6**, as opposed to the secondary coumarins **1–5**, this reaction would be promoted by three effects: firstly, the tertiary coumarin PPG has six β-protons available for deprotonation; secondly the elimination results in a double bond with a higher degree of substitution, making it more stable; thirdly, the increased steric bulk on the α-carbon resulting from the two methyl groups could potentially decrease the rate of the competing process, *i.e.* the water trapping of the cation.

We hypothesized that this new CIP escape mechanism would be an intramolecular -or 'intra-ion pair'-process, circumventing the need for diffusion of both ions in the CIP. Being liberated from diffusion-dependency, we hypothesized that for tertiary coumarin, the k_2 CIP escape energy barrier, and therefore the QY of **6**, would not be affected by solvent polarity and payload size/hydrophobicity (Fig. 2b). Hypothetically, the QY of tertiary coumarin **6** would be significantly more independent from these factors than that of diffusion-dependent PPGs **1–5**.

Throughout this paper, we measure the QYs of the PPGs using UV-Vis spectroscopy, following the consumption of the PPG substrate upon irradiation. Given that CIP recombination (k_{-1}) happens on the nanosecond time-scale,[34] it is undetectable by our spectrophotometer and CIP recombination events will appear as the substrate remaining intact. Only when the CIP successfully undergoes CIP escape (k_2) the substrate will be consumed. Therefore, through following the efficiency of substrate conversion (*i.e.* the QY) the efficiency of CIP escape is also captured.

Results and discussion

The effect of solvent polarity

We set out to experimentally study the difference between the two CIP escape mechanisms regarding their susceptibility to

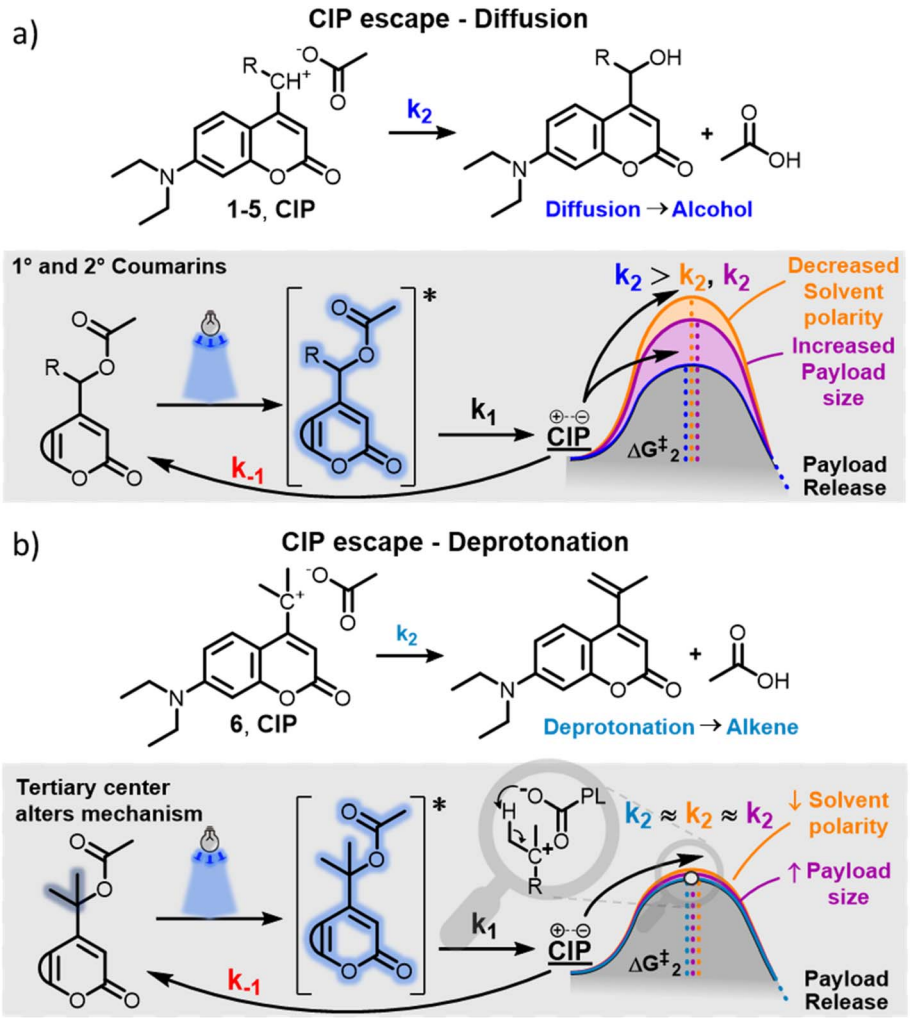

Fig. 2 (a) The conventional mechanism of CIP escape, displayed by coumarins **1–5**. A schematic representation of the energy barriers of CIP escape for diffusion-dependent PPGs, illustrating the dependency of the barrier height on solvent polarity and nature of the payload. (b) Tertiary coumarin **6** displayed the formation of an alkene upon irradiation in water. A hypothetical schematic representation of the energy diagram of the photolysis mechanism for tertiary coumarin, illustrating the expected independence of the CIP escape barrier height on these factors due to the intramolecular nature of this step, not relying on CIP diffusion.

solvent polarity in an experiment in which different mixtures of water and organic solvents were prepared to provide a range of different overall polarities. As the organic solvent, THF was chosen, based on its relatively low polarity and miscibility with water. The quantum yield (QY) of prenyl-coumarin **5** (a PPG depending on diffusion) was measured in solvent mixtures with differing water/THF ratios (Fig. 3b, black line). The QY of **5** was strongly affected by solvent polarity, showing a greater than 3-fold drop in QY over the measured solvent ratios. Gratifyingly, the QY of tertiary coumarin **6** was unaltered by the addition of the nonpolar THF (Fig. 3b, red line), and therefore independent of overall solvent polarity. These results convincingly indicate that, while solvent polarity is crucial for retaining the QY of diffusion-dependent PPGs, for tertiary coumarin **6** solvent polarity minimally affects its QY, a result likely originating from the unaltered height of the k_2 CIP escape barrier caused by the diffusion-independent nature of this step.

In a similar fashion, the photochemical QY of prenyl-coumarin **5** was also strongly influenced by the addition of other organic solvents (Fig. 3c, grey bars). The addition of ethanol already lowered the photochemical QY of **5** by 60%, while even less polar solvents further lowered its QY (Fig. 3c, grey bars). As expected, the same solvents had a minimal effect on the QY of tertiary coumarin **6** (Fig. 3c, red bars), hypothetically due to the solvent independent nature of its intramolecular CIP escape mechanism. Even the addition of comparatively apolar solvents such as dioxane showed a negligible effect on the QY of **6**, and **6** could remarkably also be uncaged with identical efficiency in pure methyl *tert*-butyl ether (MTBE) (Fig. 3c, red bars). Unexpectedly, methanol and MeCN negatively affected the QY of **6** to a certain extent, despite their relatively high polarity.

Having established that the solvent polarity drastically influences the QY of diffusion-dependent PPG **5**, we further compared the influence of the ionic strength on the uncaging

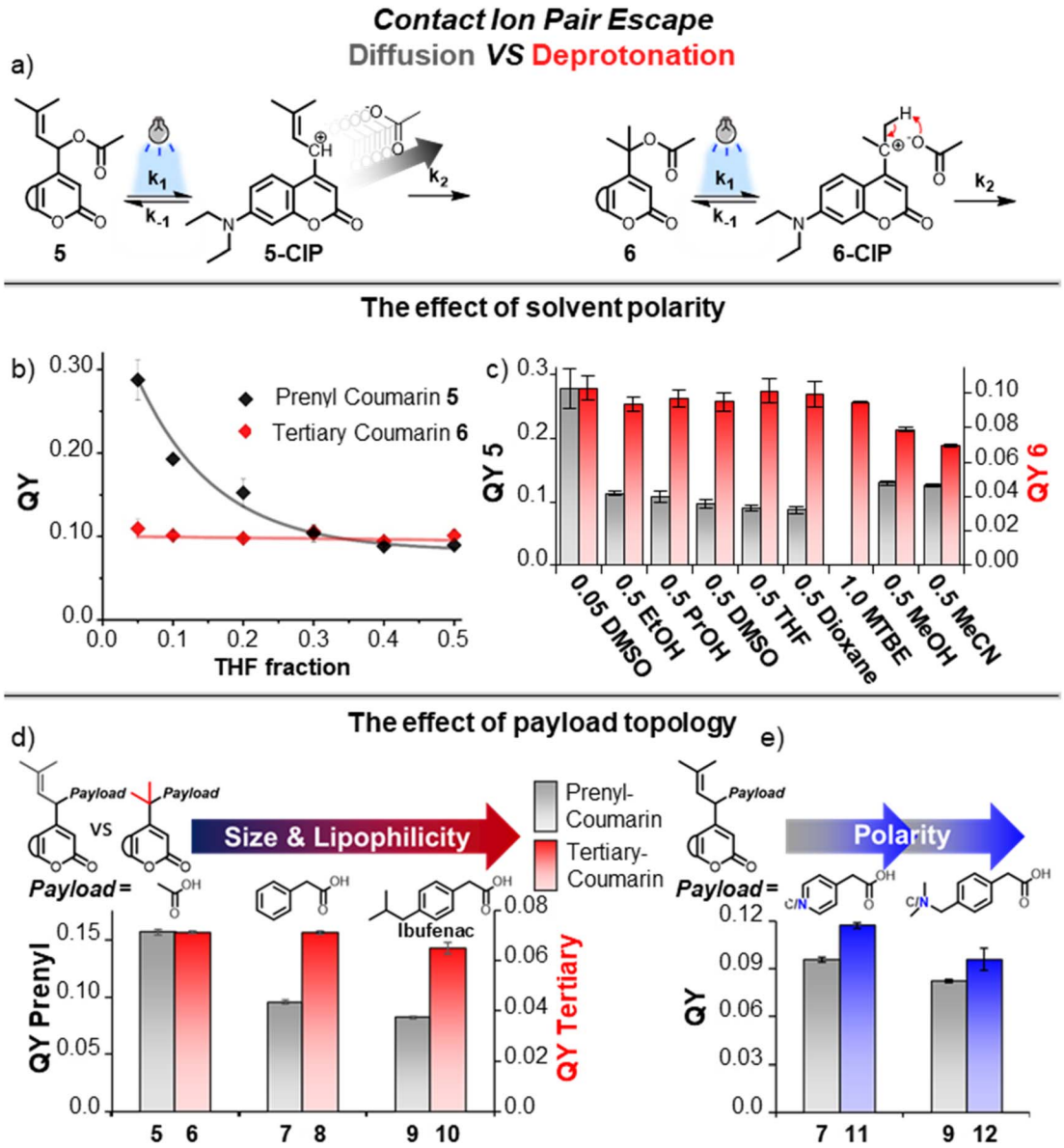

Fig. 3 (a) Schematic representation of both CIP escape mechanisms: conventional diffusion of the CIP and deprotonation undergone by tertiary-coumarin. (b) Quantum yields of photolysis of coumarins **5** and **6** (60 μM, 25 °C) in a water/THF mixture. The *x*-axis reports the volume fraction of THF in water (*e.g.*, a volume fraction of 0.5 represents a 1 : 1 mixture (v/v) of THF in water). (c) Quantum yields of photolysis of coumarins **5** (grey bars) and **6** (red bars) in various solvent mixtures. Reported is the volume fraction of organic solvent in water (QY measured at 60–50 μM, 25 °C). (d) Photolysis QYs of coumarins **5**–**10** (50 μM, water/MeCN 65 : 35, 25 °C). (e) Photolysis QYs of coumarin-PPGs **7**, **9**, **11** and **12** bearing phenylacetic acid/Ibufenac payloads (grey bars) or their nitrogen-containing analogues (blue bars) (50 μM, water/MeCN 65 : 35, 25 °C). For all QYs the averages and SD-values of triplicate measurements are reported.

efficiency of PPGs **5** and **6**. We have chosen lithium perchlorate to control the ionic strength of the solution, since the perchlorate anion is non-nucleophilic, very weakly basic and also photochemically innocent. Especially the last aspect is of crucial importance, as illustrated by the difference in uncaging rates between the heterolytic PPG system Cy7-PPG derived from cationic heptamethine cyanine dyes,[20] which we engineered to contain chloride as the counteranion to the cationic photocage, and its iodide salt counterpart reported by Stacko *et al.*[53] This comparison reveals the non-innocent photochemical nature of the iodide counterion, which promotes oxygen-dependent processes, an effect well-known in photodynamic therapy.[54,55] Interestingly, we have not observed any influence of the increase of ionic strength on the photouncaging efficiency of both PPGs **5** and **6**, indicating that for both PPGs the process is independent on the presence of non-reactive ions (see ESI Section 3.5†).

The effect of payload topology

To study the effect of payload topology on the QY of the PPGs with two different CIP escape mechanisms, we loaded both prenyl- and tertiary-coumarin with lipophilic payloads, larger

than acetic acid. We hypothesized that, due to their size, these larger payloads will feature a higher diffusion barrier from the CIP intermediate as compared to acetic acid, and therefore PPGs bearing these payloads should have a lower QY of uncaging due to an increased k_2 barrier. In a polar environment such as water, we expected payloads with increased lipophilicity to also feature an increased k_2 barrier in a similar fashion. From the CIP intermediate, the separation of two lipophilic components in water will hypothetically be more energetically costly than the separation of polar components, and therefore a higher diffusion barrier is expected. Since the uncaging of tertiary coumarin does not depend on diffusion, we were curious to see how size and lipophilicity would affect the photochemical QY of tertiary-coumarin as compared to a diffusion-dependent coumarin.

Phenylacetic acid and Ibufenac were chosen as the larger payloads with increasing size and lipophilicity. Both these payloads are (phenyl)acetic acid analogues and are expected to have highly similar pK_a values. This is crucial because payloads with a lower pK_a value will stabilize the anionic component of the CIP intermediate and increase the QY through altering the k_1 and k_{-1} energy barriers.[33,48] Choosing payloads with (near) identical pK_a allowed us to achieve isolated alteration of the k_2 barrier, and therefore study its effect on the QY.

Steglich esterification of the carboxylic acids with prenyl-coumarin alcohol yielded prenyl-coumarins **7** and **9** bearing the two lipophilic payloads (Fig. 3d). For tertiary coumarin, the increased steric hindrance required longer reaction times at elevated temperature of the tertiary alcohol with the anhydrides of the respective payloads, to yield tertiary coumarins **8** and **10** (Fig. 3d). The quantum yields of photolysis of coumarins **5–10** were determined in a water/MeCN mixture. For diffusion-dependent prenyl-coumarin PPG (Fig. 3d, grey bars), the larger phenylacetic acid payload resulted in a significant decrease in its QY, presumably through increasing the diffusion k_2 CIP escape barrier (Fig. 3d, **7**). For prenyl-coumarin loaded with the Ibufenac payload (Fig. 3d, **9**) the decrease in QY was even more pronounced (Fig. 3d, **5** *vs.* **9**). The QY of tertiary coumarin uncaging was affected minimally by the increased size of its payload (Fig. 3d, red bars **6**, **8**, **10**). No decrease in QY was found when moving from an acetic acid payload to the larger lipophilic phenylacetic acid payload (Fig. 3d, **6** *vs.* **8**), while an Ibufenac payload minimally lowered the QY (Fig. 3d, **10**). These results demonstrate the contrast between both CIP escape mechanisms, and illustrate that for tertiary coumarin uncaging does not depend on diffusion of both ions in the CIP, and therefore no relationship is found between the size or hydrophobicity of these ions and the photolysis QY. In contrast, for a PPG employing the conventional diffusion dependent CIP escape, these factors influence the QY significantly.

As the size of the payloads increases in the order acetic acid – phenylacetic acid – Ibufenac, so does their lipophilicity. Therefore, using these payloads alone, the combined influence of these two factors on the QY cannot be separated, and no conclusion can be made whether only one of them contributes to the drop in QY, or both. Therefore, we attempted to separate these factors through introducing polarity into the payloads, while keeping the size unaffected. We loaded prenyl-coumarin with aza-analogues of phenylacetic acid and Ibufenac (Fig. 3e, **11** and **12**, respectively). While being very similar in size, the polarity of these payloads differs extensively. In agreement with our rationale regarding payload polarity and diffusion barrier height, for both payloads the introduction of a nitrogen atom increased the QY as compared to their carbon-analogues (Fig. 3e, blue bars compared to grey bars). These results demonstrate that irrespective of size, payload polarity influences the height of the diffusion barrier and the introduction of polarity has a favorable effect on the QY, likely through the reduction of this barrier. An interplay between both payload size and polarity determines the overall height of the k_2 barrier and therefore both factors influence the final photochemical QY.

Overall, the results described in this section demonstrate the shortcomings of conventional diffusion-dependent heterolytic PPGs. The QYs of these PPGs can be strongly negatively affected by factors such as payload topology and polarity of the environment. The deprotonation mechanism – an intramolecular type of CIP escape – showcases itself as being superior, illustrated by the QY of tertiary coumarin that is minimally influenced by these factors. Furthermore, the tertiary coumarin PPGs **6**, **8** and **10** showed excellent hydrolytic stability. No hydrolysis products were observed after incubation at 25 °C in water/DMSO mixtures (see ESI Section 3.10†). Lastly, uncaging chemical yields were determined for model compounds **5–8**, that all showed high chemical yields ranging from 90–100% (see ESI Section 3.9†).

Including the CIP escape k_2 barrier in the analysis

Despite tertiary-coumarin's different mechanism and different response to payload size and solvent polarity, we set out to include it in our previous analysis that correlates the QY of the diffusion dependent PPGs to the energy barriers. This analysis[48] relied on the study of k_1 and k_{-1}, not including k_2. From the strong correlation of the QYs of diffusion dependent coumarins **1–5** to the ratio of k_1/k_{-1} alone, we conclude that their k_2 diffusion barrier must be energetically nearly identical. This seems reasonable, since all these compounds have similar molecular topologies of the cationic component of the formed CIP and an identical anionic component (*i.e.* the acetate payload). However, we previously reported that tertiary coumarin **6** was an outlier in this linear correlation. Logically, the alternative mechanism (deprotonation) of CIP escape that PPG **6** displayed is the likely cause of its QY not fitting the linear correlation in Fig. 1c. Since its QY is higher than can be explained by its k_{-1}/k_1 energy barrier ratio, it must be concluded that the deprotonation k_2 barrier for **6** is lower than the conventional CIP diffusion and water capture k_2 barrier.

To expand our analysis that correlates photolysis QYs with the individual reaction barriers, regardless of the mechanism of CIP escape, we set out to include the mechanism of CIP escape k_2 barrier in our analysis. Given that k_2, like k_1, is a productive step in the photolysis reaction, we included the value of the associated energy barrier into the denominator to reach a fraction that includes the height of all three barriers (eqn (1)

(right)). This energy barrier ratio is related to the probability that a compound undergoing photoheterolysis travels its energy landscape productively. Therefore, we believed it should correlate to the photolysis QY as well. Eqn (1) shows the previously published fraction used for correlating the QY to the energy barriers (left)[48] and a new energy barrier ratio that takes into account all steps in the photolysis process and respective energy barriers (right)

$$\mathrm{QY} \propto \frac{\Delta G^{\ddagger}_{k-1}}{\Delta G^{\ddagger}_{k_1}} \rightarrow \mathrm{QY} \propto \frac{\Delta G^{\ddagger}_{k-1}}{\Delta G^{\ddagger}_{k_1} \times \Delta G^{\ddagger}_{k_2}} \quad (1)$$

Similar to our previous analysis,[48] we sought out to compute all excited state energy barriers by TD-DFT calculations. For these calculations, we made the assumption that any productive photochemical processes would be occurring from the first singlet excited state (S_1), which is consistent with what is known of coumarin-PPG photoheterolysis.[33,48] TD-DFT has been previously used to compute photoheterolysis barriers on both the S_1 and T_1 excited state energy landscapes of coumarin- and BODIPY-PPGs.[20,32,41,48,56] It should be noted that, while heterolysis (k_1) occurs in S_1,[33] relaxation to S_0 might happen at any time after CIP formation. Therefore, the extent to which CIP recombination (k_{-1}) and CIP escape (k_2) occur at S_1 -if at all- is unclear. However, using TD-DFT we were unable to find a stable CIP in S_0 and therefore unable to perform any computations on the k_{-1} and k_2 energy barriers in S_0. Therefore, our analyses are constrained to photochemical processes on the S_1 potential energy landscape, and are to be seen as an approximation of the actual photolysis energy landscape. Nonetheless, the strong correlation of the k_{-1}/k_1 energy barrier ratio to the photolysis QY obtained in our previous analysis[48] suggests that the computed heights of the energy barriers relative to one another among different PPGs are highly relevant.

To supplement our previous analysis that relied solely on k_1 an k_{-1}, the k_2 barrier for the deprotonation that is proposed for the tertiary PPG **6** was also computed by TD-DFT in the first singlet excited state, and predicted to be 9.4 kcal mol^{-1} (see ESI Section 4†). For the other PPGs **1–5** that relied on CIP escape *via* diffusion of the chromophore cation and payload anion and water trapping, their k_2 diffusion energy barriers could not be computed by TD-DFT. Therefore, we set out to numerically approximate their diffusion barrier using eqn (1). In this equation, we filled in the DFT calculated 9.4 kcal mol^{-1} for the k_2 barrier height of **6**. The value of the acetate diffusion barrier for all other coumarins was left as a variable. Through maximizing R^2 numerically (Fig. 4), a k_2 barrier height for diffusion of ~14.6 kcal mol^{-1} was obtained.

Additionally, performing the same analysis without including the calculated k_1 heterolysis barriers also gave an excellent correlation with the QY, resulting in an R^2 of 0.9975. Using this method, a slightly lower k_2 acetate diffusion barrier was found (see ESI, Section 5†).

The obtained correlation of the ratio of the photolysis energy barriers with the QY is strong ($R^2 > 0.99$). Still, it has to be noted that the predicted height of the k_2 diffusion barrier relies on the accuracy of all energy barriers computed by TD-DFT, which as discussed above, were all performed exclusively for the first singlet excited state. Therefore, the obtained diffusion barrier height of 14.6 kcal mol^{-1} should be seen as a qualitative estimation, rather than a quantitative one.

Predicting a QY – reliability of the analysis

Our analysis resulted in an exponential relationship between the QY of the coumarin PPGs and an energy barrier ratio that included all three barriers, out of which the following formula was derived (eqn (2)):

$$\mathrm{QY} = 0.0143 \times \mathrm{e}^{19.1x} \quad \text{in which} \quad x = \frac{\Delta G^{\ddagger}_{k-1}}{\Delta G^{\ddagger}_{k_1} \times \Delta G^{\ddagger}_{k_2}} \quad (2)$$

Eqn (2) shows the formula describing the relationship between the QY of coumarin PPGs **1–6** and the energy barrier ratio. This formula connects the QY to the photolysis energy barriers alone, and does not account for any other photophysical processes that may occur after excitation. For example, eqn (2) does not account for excited state relaxation processes such as fluorescence and internal conversion, the rate of which do influence the QY of competing photolysis. If the rates of these processes would differ significantly between each coumarin variant **1–6**, we would be unable to correlate the photolysis QYs solely to the computed photolysis energy barrier ratio. However, judging from the experimentally obtained strong correlation (Fig. 4 and previous work[48]), we conclude that it is likely not the case. This is supported by the fluorescence

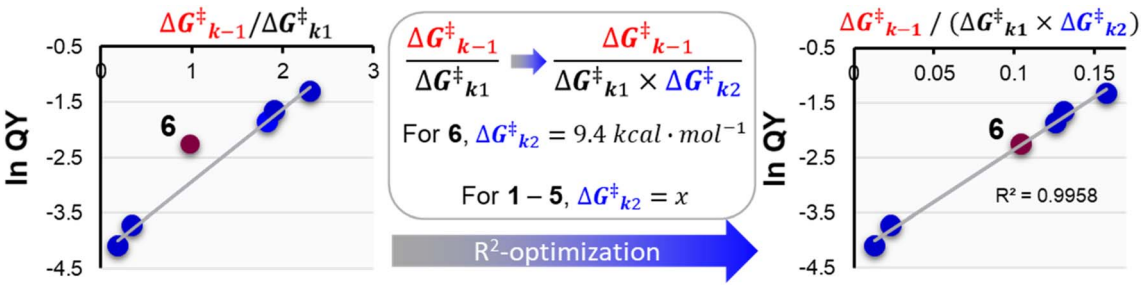

Fig. 4 Exponential plot of the QY of photolysis *versus* the $\Delta G^{\ddagger}_{k-1}/\Delta G^{\ddagger}_{k_1}$ energy barrier ratio as reported in our previous analysis[48] (left). Including $\Delta G^{\ddagger}_{k_2}$ in the energy barrier ratio allows for an estimation of the diffusion barrier through R^2-optimization (right).

QYs we determined for the parent alcohols of **1–6**, that lack the acetic acid payload and therefore the PPG functionality itself. These alcohols all displayed similar fluorescence QYs, ranging from 9–12% (see ESI Section 3.8†). Therefore, interestingly, modification of the coumarin alpha-carbon appears to not affect the rate of fluorescence -and likely other photophysical processes- to a significant extent. A possible explanation for this could be that the performed synthetic modifications do not result in alteration of the chromophore itself, but importantly stabilize the cation that is generated *exclusively after photoheterolysis* and not in any of the other competing processes.

Since our analysis solely focused on the photolysis barriers, we were interested in testing the reliability of the newly found correlation. We hypothesized that if the obtained formula (eqn (2)) adequately describes the system, it could allow us to predict the photolysis QY of an isotopologue PPG of **6**. The compound we designed for this purpose was deuterated-coumarin **6-D$_6$** (Fig. 5a). Being a tertiary coumarin, we expected it to undergo deprotonation as CIP escape mechanism. And by virtue of being an isotopologue of **6**, **6-D$_6$** would have identical (photo)-chemical and topological properties as **6**. The primary isotope effect of deuteron rather than proton abstraction would result in a larger k_2 barrier for **6-D$_6$** than for tertiary coumarin **6**, effectively resulting in a third k_2 barrier (diffusion, H^+-abstraction, D^+-abstraction). DFT calculations confirmed this, yielding a predicted energy barrier of deuteron abstraction of 11.5 kcal-mol^{-1}, as compared to 9.4 kcal mol^{-1} for proton abstraction of **6**. Eqn (3) shows the energy barrier ratio 'x' as calculated for compound **6-D$_6$** based on the DFT-calculated height of the three energy barriers, and the predicted QY of **6-D$_6$** through filling in 'x' in the previously established formula correlating the QY to the energy barrier ratio.

$$\text{For } \textbf{6-D6}: \; x = \frac{G^{\ddagger}_{k-1}}{\Delta G^{\ddagger}_{k_1} \times \Delta G^{\ddagger}_{k_2}} = 0.0836$$
$$\text{QY} = 0.0143 \times e^{19.1x} = \mathbf{0.0706} \qquad (3)$$

Feeding the DFT calculated energy barriers for k_1, k_{-1} and k_2 to eqn (2) allowed us to predict the photolysis QY of **6-D$_6$** at 7.06% (eqn (3)), roughly 30% lower than the QY of its protonated analogue **6**. To our delight, experimental determination of the QY yielded an almost identical number of 7.0 ± 0.4%.

The fact that eqn (2) is highly predictive indicates that our analysis comprises the most important factors that determine coumarin PPG QY. We expect equations analogous to eqn (2) to allow for the optimization of QY in the design of new PPGs, through revealing trends correlating PPG design to expected QY. These trends can be established using acetate as a model cargo, but we expect them to be transferable to other types of cargos with different diffusion barriers. Our general approach could be expanded to other heterolytic PPGs and aid in their efficient design, bearing in mind that the specific equation would have to be adapted due to those PPGs having different rates of competing photophysical processes.

Payload topology becomes crucial for PPGs with high uncaging quantum yield

When studying the effect of payload topology on the QY of conventional primary coumarin, we did not find a significant difference in QY between primary coumarins bearing a phenylacetic acid or acetic acid payload (see ESI Section 3.5†). While initially these results were puzzling, they can be rationalized by looking at the relationship between QY and the energy barrier ratio. Since their relationship is exponential, when a productive energy barrier goes up, a much larger decrease in QY is expected for PPGs in the high QY region. For example, assuming that a payload change from acetic acid to a larger payload (Fig. 6, **1-AA/LP** and **5-AA/LP**) would increase the k_2 barrier of a diffusion-dependent PPG 1.5 fold, for prenyl coumarin a ~20% loss in QY is predicted (Fig. 6, predicted QY of **5-AA** *vs.* **5-LP**), whereas for primary coumarin the same barrier increase would only result in a 0.1% loss (Fig. 6, predicted QY of **1-AA** *vs.* **1-LP**).

Therefore, when scientific fields employing PPGs as photochemical tools move towards the use of more efficient PPGs that still rely on diffusion as CIP escape, the size of the payload becomes a highly important factor and a larger payload will likely lower the QY significantly, negating the efforts of QY optimization. Since almost all relevant payloads are larger than acetic acid (note that most payloads used in the field of

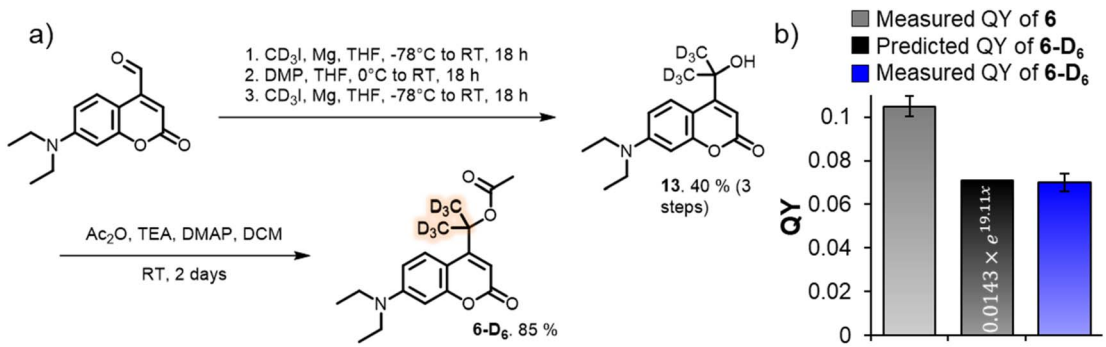

Fig. 5 (a) Synthetic scheme for the formation of deuterated tertiary coumarin **6-D$_6$**. (b) Predicted QY of coumarin **6-D$_6$** using eqn (2), and measured QY of **6-D$_6$** (55 μM, water 2.7% MeCN, 25 °C, shown is the average and SD-value of a triplicate measurement).

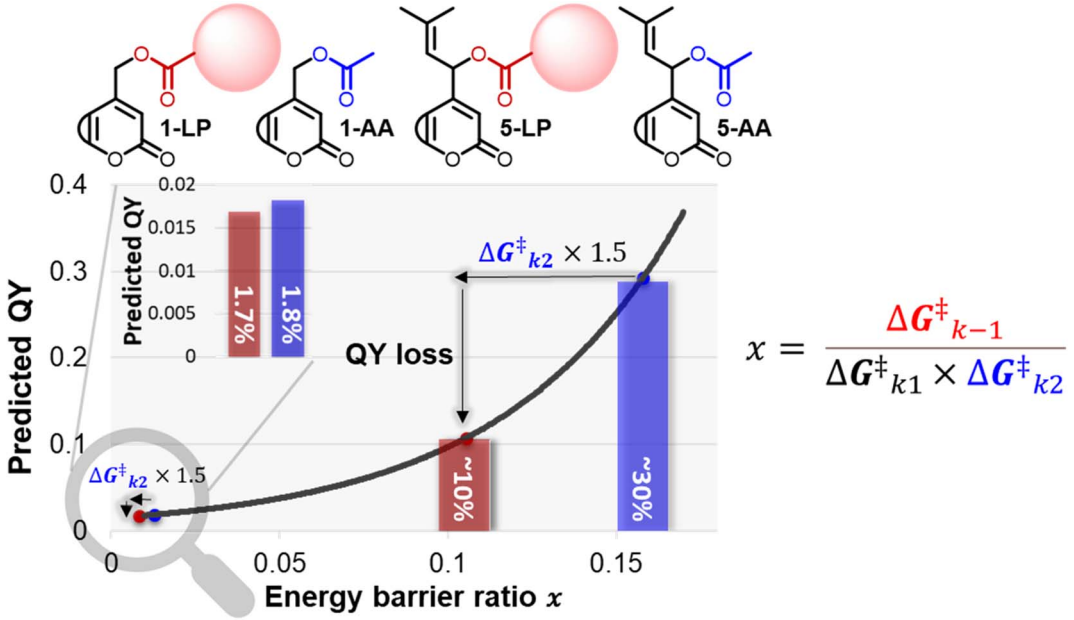

Fig. 6 Plot of eqn (2), displaying the energy barrier ratio (x-axis) *vs.* the QY (y-axis). An increase of the k_2 barrier height is predicted to lower the QY of efficient diffusion-dependent PPGs drastically (prenyl-coumarin with acetic acid *vs.* a large payload (red sphere)). The same relative increase of the k_2 barrier height has a minimal effect on the QY of inefficient PPGs (*e.g.*, primary coumarin).

photopharmacology are larger bioactive compounds) this effect for diffusion-dependent PPGs will become highly relevant. It emphasizes the importance of engineering the CIP escape mechanism k_2 and further highlights the advantage that PPGs with an intramolecular type of CIP escape – like **6**, that circumvent these issues- have over conventional diffusion-dependents PPGs, most notably when moving towards higher QYs. For example, for the field of photopharmacology, the development of *water-soluble PPGs with an intramolecular type of CIP escape and a high QY* will be a major step forward.

Conclusion and outlook

In this study, we present an outline of the factors that determine the photochemical QY of coumarin PPGs, a fundamental member of the class of heterolytic PPGs. For the first time, we describe the key importance of the k_2 CIP escape barrier, highlighting the practical differences between two types of CIP escape: *diffusion* and *intramolecular deprotonation by the payload.* We demonstrate that the QY of PPGs that undergo diffusion-dependent CIP escape can be strongly influenced by solvent polarity and payload topology. In contrast, the intramolecular nature of CIP escape for tertiary coumarin renders its QY highly predictable and minimally influenced by solvent polarity and payload topology. We observed a strong correlation of the QYs of all PPGs with an energy barrier ratio that included all three energy barriers in the coumarin photolysis reaction and estimated a k_2 diffusion barrier height for an acetate payload. The high reliability of the analysis was demonstrated through the prediction of a QY of a new PPG, illustrating that the coumarin photolysis QY can be explained to a large extent through analyzing the photolysis energy barriers exclusively. Furthermore, the accurate prediction of the QY of **6-D$_6$** strongly supports the proposed deprotonation CIP escape mechanism of tertiary coumarins and provides a justification for the observed independence of the QY of **6** to solvent polarity and payload topology. The insights obtained here can most likely be applied to other members of the heterolytic class of PPGs as well[42] since the members of this class share the same mechanism, illustrating the great value of developing the understanding of heterolytic PPG photochemistry through synthetically more accessible and easily modifiable coumarins. Perhaps most strikingly, our findings highlight the advantage an intramolecular type of CIP escape has over a diffusion-dependent CIP escape pathway, especially at high QY. Applying these principles to more red-shifted heterolytic PPGs would be an exciting future step. Some of these PPGs already display CIP escape mechanisms that appear of intramolecular nature,[42,50] or feature a tertiary center at the alpha carbon,[20] suggesting that the principles presented in this paper could be applied across the wavelength spectrum to yield superior heterolytic PPGs.

Data availability

We provide an extensive ESI† file that includes all relevant data such as synthetic methods, NMR spectra, uncaging QY measurements, fluorescence QY measurements, NMR spectra of uncaging and all computational data.

Author contributions

A. M. S. conceived the study in collaboration with G. A. A. M. S. performed the synthesis and photochemical measurements. G.

A. performed the DFT calculations. W. S. and B. L. F. assisted in conceiving the study and supervised the project.

Conflicts of interest

There are no conflicts to declare.

Acknowledgements

The authors are grateful for the generous funding support to G. A. (EMBO LTF-232-2020 Postdoctoral Fellowship), and to B. L. F. (ERC Advanced Investigator Grant No. 694345; and the Ministry of Education, Culture and Science of The Netherlands Gravitation Program No. 024.001.035). The authors are grateful to J. L. Sneep for collecting high-resolution mass-spectrometry data for all newly reported compounds. The authors thank the Center for Information Technology of the University of Groningen for their support and for providing access to the Peregrine high-performance computing cluster.

References

1 W. A. Velema, W. Szymanski and B. L. Feringa, Photopharmacology: Beyond Proof of Principle, *J. Am. Chem. Soc.*, 2014, **136**(6), 2178–2191, DOI: **10.1021/ja413063e**.

2 J. Broichhagen, J. A. Frank and D. Trauner, A Roadmap to Success in Photopharmacology, *Acc. Chem. Res.*, 2015, **48**(7), 1947–1960, DOI: **10.1021/acs.accounts.5b00129**.

3 C. Brieke, F. Rohrbach, A. Gottschalk, G. Mayer and A. Heckel, Light-Controlled Tools, *Angew. Chem. Int., Ed.*, 2012, **51**(34), 8446–8476, DOI: **10.1002/anie.201202134**.

4 K. Long, H. Han, W. Kang, W. Lv, L. Wang, Y. Wang, L. Ge and W. Wang, One-Photon Red Light-Triggered Disassembly of Small-Molecule Nanoparticles for Drug Delivery, *J. Nanobiotechnol.*, 2021, **19**(1), 357, DOI: **10.1186/s12951-021-01103-z**.

5 M. Ricart-Ortega, J. Font and A. Llebaria, GPCR Photopharmacology, *Mol. Cell Endocrinol.*, 2019, **488**, 36–51, DOI: **10.1016/j.mce.2019.03.003**.

6 M. J. Hansen, W. A. Velema, M. M. Lerch, W. Szymanski and B. L. Feringa, Wavelength-Selective Cleavage of Photoprotecting Groups: Strategies and Applications in Dynamic Systems, *Chem. Soc. Rev.*, 2015, **44**(11), 3358–3377, DOI: **10.1039/C5CS00118H**.

7 P. Štacko and T. Šolomek, Photoremovable Protecting Groups: Across the Light Spectrum to Near-Infrared Absorbing Photocages, *Chimia*, 2021, **75**(10), 873–881, DOI: **10.2533/chimia.2021.873**.

8 R. Weinstain, T. Slanina, D. Kand and P. Klán, Visible-to-NIR-Light Activated Release: From Small Molecules to Nanomaterials, *Chem. Rev.*, 2020, **120**(24), 13135–13272, DOI: **10.1021/acs.chemrev.0c00663**.

9 I. M. Welleman, M. W. H. Hoorens, B. L. Feringa, H. H. Boersma and W. Szymański, Photoresponsive Molecular Tools for Emerging Applications of Light in Medicine, *Chem. Sci.*, 2020, **11**(43), 11672–11691, DOI: **10.1039/D0SC04187D**.

10 A. E. Mangubat-Medina and Z. T. Ball, Triggering Biological Processes: Methods and Applications of Photocaged Peptides and Proteins, *Chem. Soc. Rev.*, 2021, **50**(18), 10403–10421, DOI: **10.1039/D0CS01434F**.

11 K. Long, Y. Yang, W. Lv, K. Jiang, Y. Li, A. C. Y. Lo, W. C. Lam, C. Zhan and W. Wang, Green Light-Triggered Intraocular Drug Release for Intravenous Chemotherapy of Retinoblastoma, *Adv. Sci.*, 2021, **8**(20), 2101754, DOI: **10.1002/advs.202101754**.

12 Y. Li, W. Lv, L. Wang, Y. Zhang, L. Yang, T. Wang, L. Zhu, Y. Wang and W. Wang, Photo-Triggered Nucleus Targeting for Cancer Drug Delivery, *Nano Res.*, 2021, **14**(8), 2630–2636, DOI: **10.1007/s12274-020-3264-0**.

13 T. Šolomek, J. Wirz and P. Klán, Searching for Improved Photoreleasing Abilities of Organic Molecules, *Acc. Chem. Res.*, 2015, **48**(12), 3064–3072, DOI: **10.1021/ACS.ACCOUNTS.5B00400**.

14 C. G. Bochet, Photolabile Protecting Groups and Linkers, *J. Chem. Soc., Perkin Trans. 1*, 2002, **2**, 125–142, DOI: **10.1039/b009522m**.

15 N. Hoffmann, Photochemical Reactions as Key Steps in Organic Synthesis, *Chem. Rev.*, 2008, **108**(3), 1052–1103, DOI: **10.1021/cr0680336**.

16 R. K. Deshpande, G. I. N. Waterhouse, G. B. Jameson and S. G. Telfer, Photolabile Protecting Groups in Metal–Organic Frameworks: Preventing Interpenetration and Masking Functional Groups, *Chem. Commun.*, 2012, **48**(10), 1574–1576, DOI: **10.1039/C1CC12884A**.

17 G. C. R. Ellis-Davies, Caged Compounds: Photorelease Technology for Control of Cellular Chemistry and Physiology, *Nat. Methods*, 2007, **4**(8), 619–628, DOI: **10.1038/nmeth1072**.

18 K. Hüll, J. Morstein and D. Trauner, In Vivo Photopharmacology, *Chem. Rev.*, 2018, **118**(21), 10710–10747, DOI: **10.1021/acs.chemrev.8b00037**.

19 M. M. Lerch, M. J. Hansen, G. M. van Dam, W. Szymanski and B. L. Feringa, Emerging Targets in Photopharmacology, *Angew. Chem., Int. Ed.*, 2016, 10978–10999, DOI: **10.1002/anie.201601931**.

20 G. Alachouzos, A. M. Schulte, A. Mondal, W. Szymanski and B. L. Feringa, Computational Design, Synthesis, and Photochemistry of Cy7-PPG, an Efficient NIR-Activated Photolabile Protecting Group for Therapeutic Applications, *Angew. Chem., Int. Ed.*, 2022, **61**(27), e202201308, DOI: **10.1002/anie.202201308**.

21 C. Bier, D. Binder, D. Drobietz, A. Loeschcke, T. Drepper, K.-E. Jaeger and J. Pietruszka, Photocaged Carbohydrates: Versatile Tools for Controlling Gene Expression by Light, *Synthesis*, 2016, **49**(1), 42–52, DOI: **10.1055/s-0035-1562617**.

22 Q. Huang, C. Bao, W. Ji, Q. Wang and L. Zhu, Photocleavable Coumarin Crosslinkers Based Polystyrene Microgels: Phototriggered Swelling and Release, *J. Mater. Chem.*, 2012, **22**(35), 18275–18282, DOI: **10.1039/c2jm33789d**.

23 S. P. A. Fodor, J. L. Read, M. C. Pirrung, L. Stryer, A. T. Lu and D. Solas, Light-Directed, Spatially Addressable Parallel

Chemical Synthesis, *Science*, 1991, **251**(4995), 767–773, DOI: 10.1126/science.1990438.

24 S. Weis, Z. Shafiq, R. A. Gropeanu and A. Del Campo, Ethyl Substituted Coumarin-4-Yl Derivatives as Photoremovable Protecting Groups for Amino Acids with Improved Stability for SPPS, *J. Photochem. Photobiol. A Chem.*, 2012, **241**, 52–57, DOI: 10.1016/j.jphotochem.2012.05.014.

25 G. Bassolino, C. Nançoz, Z. Thiel, E. Bois, E. Vauthey and P. Rivera-Fuentes, Photolabile Coumarins with Improved Efficiency through Azetidinyl Substitution, *Chem. Sci.*, 2018, **9**(2), 387–391, DOI: 10.1039/C7SC03627B.

26 M. Bojtár, A. Kormos, K. Kis-Petik, M. Kellermayer and P. Kele, Green-Light Activatable, Water-Soluble Red-Shifted Coumarin Photocages, *Org. Lett.*, 2019, **21**(23), 9410–9414, DOI: 10.1021/acs.orglett.9b03624.

27 A. Gandioso, S. Contreras, I. Melnyk, J. Oliva, S. Nonell, D. Velasco, J. García-Amorós and V. Marchán, Development of Green/Red-Absorbing Chromophores Based on a Coumarin Scaffold That Are Useful as Caging Groups, *J. Org. Chem.*, 2017, **82**(10), 5398–5408, DOI: 10.1021/acs.joc.7b00788.

28 M. J. Hansen, F. M. Feringa, P. Kobauri, W. Szymanski, R. H. Medema and B. L. Feringa, Photoactivation of MDM2 Inhibitors: Controlling Protein-Protein Interaction with Light, *J. Am. Chem. Soc.*, 2018, **140**(41), 13136–13141, DOI: 10.1021/jacs.8b04870.

29 K. Sitkowska, B. L. Feringa and W. Szymański, Green-Light-Sensitive BODIPY Photoprotecting Groups for Amines, *J. Org. Chem.*, 2018, **83**(4), 1819–1827, DOI: 10.1021/acs.joc.7b02729.

30 E. Contreras-García, C. Lozano, C. García-Iriepa, M. Marazzi, A. H. Winter, C. Torres and D. Sampedro, Controlling Antimicrobial Activity of Quinolones Using Visible/NIR Light-Activated BODIPY Photocages, *Pharmaceutics*, 2022, **14**(5), 1070, DOI: 10.3390/pharmaceutics14051070.

31 S. Leichnitz, K. C. Dissanayake, A. H. Winter and P. H. Seeberger, Photo-Labile BODIPY Protecting Groups for Glycan Synthesis, *Chem. Commun.*, 2022, **58**(75), 10556–10559, DOI: 10.1039/d2cc03851j.

32 D. Kand, P. Liu, M. X. Navarro, L. J. Fischer, L. Rousso-Noori, D. Friedmann-Morvinski, A. H. Winter, E. W. Miller and R. Weinstain, Water-Soluble BODIPY Photocages with Tunable Cellular Localization, *J. Am. Chem. Soc.*, 2020, **142**(11), 4970–4974, DOI: 10.1021/jacs.9b13219.

33 R. Schmidt, D. Geissler, V. Hagen and J. Bendig, Mechanism of Photocleavage of (Coumarin-4-Yl)Methyl Esters, *J. Phys. Chem. A*, 2007, **111**(26), 5768–5774, DOI: 10.1021/jp071521c.

34 R. Schmidt, D. Geissler, V. Hagen and J. Bendig, Kinetics Study of the Photocleavage of (Coumarin-4-Yl)Methyl Esters, *J. Phys. Chem. A*, 2005, **109**(23), 5000–5004, DOI: 10.1021/jp050581k.

35 T. Eckardt, V. Hagen, B. Schade, R. Schmidt, C. Schweitzer and J. Bendig, Deactivation Behavior and Excited-State Properties of (Coumarin-4-Yl)Methyl Derivatives. 2. Photocleavage of Selected (Coumarin-4-Yl)Methyl-Caged Adenosine Cyclic 3',5'-Monophosphates with Fluorescence Enhancement, *J. Org. Chem.*, 2002, **67**(3), 703–710, DOI: 10.1021/JO010692P.

36 B. Schade, V. Hagen, R. Schmidt, R. Herbrich, E. Krause, T. Eckardt and J. Bendig, Deactivation Behavior and Excited-State Properties of (Coumarin-4-Yl)Methyl Derivatives. 1. Photocleavage of (7-Methoxycoumarin-4-Yl) Methyl-Caged Acids with Fluorescence Enhancement, *J. Org. Chem.*, 1999, **64**(25), 9109–9117, DOI: 10.1021/jo9910233.

37 P. Klán, T. Šolomek, C. G. Bochet, A. Blanc, R. Givens, M. Rubina, V. Popik, A. Kostikov and J. Wirz, Photoremovable Protecting Groups in Chemistry and Biology: Reaction Mechanisms and Efficacy, *Chem. Rev.*, 2013, **113**(1), 119–191, DOI: 10.1021/cr300177k.

38 A. Y. Vorobev and A. E. Moskalensky, Long-Wavelength Photoremovable Protecting Groups: On the Way to in Vivo Application, *Comput. Struct. Biotechnol. J.*, 2020, **18**, 27–34, DOI: 10.1016/J.CSBJ.2019.11.007.

39 J. A. Peterson, C. Wijesooriya, E. J. Gehrmann, K. M. Mahoney, P. P. Goswami, T. R. Albright, A. Syed, A. S. Dutton, E. A. Smith and A. H. Winter, Family of BODIPY Photocages Cleaved by Single Photons of Visible/Near-Infrared Light, *J. Am. Chem. Soc.*, 2018, **140**(23), 7343–7346, DOI: 10.1021/jacs.8b04040.

40 P. P. Goswami, A. Syed, C. L. Beck, T. R. Albright, K. M. Mahoney, R. Unash, E. A. Smith and A. H. Winter, BODIPY-Derived Photoremovable Protecting Groups Unmasked with Green Light, *J. Am. Chem. Soc.*, 2015, **137**(11), 3783–3786, DOI: 10.1021/jacs.5b01297.

41 T. Slanina, P. Shrestha, E. Palao, D. Kand, J. A. Peterson, A. S. Dutton, N. Rubinstein, R. Weinstain, A. H. Winter and P. Klán, In Search of the Perfect Photocage: Structure–Reactivity Relationships in Meso -Methyl BODIPY Photoremovable Protecting Groups, *J. Am. Chem. Soc.*, 2017, **139**(42), 15168–15175, DOI: 10.1021/jacs.7b08532.

42 P. Shrestha, K. C. Dissanayake, E. J. Gehrmann, C. S. Wijesooriya, A. Mukhopadhyay, E. A. Smith and A. H. Winter, Efficient Far-Red/Near-IR Absorbing BODIPY Photocages by Blocking Unproductive Conical Intersections, *J. Am. Chem. Soc.*, 2020, **142**(36), 15505–15512, DOI: 10.1021/jacs.0c07139.

43 M. Sharma and S. H. Friedman, The Issue of Tissue: Approaches and Challenges to the Light Control of Drug Activity, *ChemPhotoChem*, 2021, 611–618, DOI: 10.1002/cptc.202100001.

44 D. C. F. Monteiro, E. Amoah, C. Rogers and A. R. Pearson, Using Photocaging for Fast Time-Resolved Structural Biology Studies, *Acta Crystallogr. D*, 2021, **77**(10), 1218–1232, DOI: 10.1107/S2059798321008809.

45 K.-Y. Chung, A. Uddin and Z. A. Page, Record Release of Tetramethylguanidine Using a Green Light Activated Photocage for Rapid Synthesis of Soft Materials, *Chem. Sci.*, 2023, **14**(39), 10736–10743, DOI: 10.1039/D3SC04130A.

46 P. Shrestha, A. Mukhopadhyay, K. C. Dissanayake and A. H. Winter, Efficiency of Functional Group Caging with Second-Generation Green- and Red-Light-Labile BODIPY

Photoremovable Protecting Groups, *J. Org. Chem.*, 2022, **87**(21), 14334–14341, DOI: **10.1021/acs.joc.2c01781**.

47 T. Šolomek, S. Mercier, T. Bally and C. G. Bochet, Photolysis of Ortho-Nitrobenzylic Derivatives: The Importance of the Leaving Group, *Photochem. Photobiol. Sci.*, 2012, **11**(3), 548–555, DOI: **10.1039/c1pp05308f**.

48 A. M. Schulte, G. Alachouzos, W. Szymański and B. L. Feringa, Strategy for Engineering High Photolysis Efficiency of Photocleavable Protecting Groups through Cation Stabilization, *J. Am. Chem. Soc.*, 2022, **144**(27), 12421–12430, DOI: **10.1021/jacs.2c04262**.

49 A. Egyed, K. Németh, T. Molnár, M. Kállay, P. Kele and M. Bojtár, Turning Red without Feeling Embarrassed-Xanthenium-Based Photocages for Red-Light-Activated Phototherapeutics, *J. Am. Chem. Soc.*, 2022, **145**(7), 4026–4034, DOI: **10.1021/jacs.2c11499**.

50 J. Chaud, C. Morville, F. Bolze, D. Garnier, S. Chassaing, G. Blond and A. Specht, Two-Photon Sensitive Coumarinyl Photoremovable Protecting Groups with Rigid Electron-Rich Cycles Obtained by Domino Reactions Initiated by a 5- Exo-Dig Cyclocarbopalladation, *Org. Lett.*, 2021, **23**(19), 7580–7585, DOI: **10.1021/ACS.ORGLETT.1C02778/SUPPL_FILE/OL1C02778_SI_001.PDF**.

51 Q. Lin, L. Yang, Z. Wang, Y. Hua, D. Zhang, B. Bao, C. Bao, X. Gong and L. Zhu, Coumarin Photocaging Groups Modified with an Electron-Rich Styryl Moiety at the 3-Position: Long-Wavelength Excitation, Rapid Photolysis, and Photobleaching, *Angew. Chem., Int. Ed.*, 2018, **57**(14), 3722–3726, DOI: **10.1002/anie.201800713**.

52 E. V. Anslyn and D. A. Dougherty, *Modern Physical Organic Chemistry*, 2006.

53 H. Janeková, M. Russo, U. Ziegler and P. Štacko, Photouncaging of Carboxylic Acids from Cyanine Dyes with Near-Infrared Light, *Angew. Chem., Int. Ed.*, 2022, **61**(33), e202204391, DOI: **10.1002/anie.202204391**.

54 C. Vieira, A. T. P. C. Gomes, M. Q. Mesquita, N. M. M. Moura, M. G. P. M. S. Neves, M. A. F. Faustino and A. Almeida, An Insight Into the Potentiation Effect of Potassium Iodide on APDT Efficacy, *Front. Microbiol.*, 2018, **9**(NOV), 415487, DOI: **10.3389/fmicb.2018.02665**.

55 M. Bispo, A. Anaya-Sanchez, S. Suhani, E. J. M. Raineri, M. López-Álvarez, M. Heuker, W. Szymański, F. R. Pastrana, G. Buist, A. R. Horswill, K. P. Francis, G. M. van Dam, M. van Oosten and J. M. van Dijl, Fighting Staphylococcus Aureus Infections with Light and Photoimmunoconjugates, *JCI Insight*, 2020, **5**(22), e139512, DOI: **10.1172/jci.insight.139512**.

56 P. Wang and C. Lim, Photolabile Protecting Groups Based on the Excited State Meta Effect: Development and Application, *Photochem. Photobiol.*, 2023, 221–234, DOI: **10.1111/php.13690**.